Repulsion by Slit and Roundabout prevents Shotgun/E-cadherin–mediated cell adhesion during *Drosophila* heart tube lumen formation

Edgardo Santiago-Martínez,[1,2] Nadine H. Soplop,[1,2] Rajesh Patel,[1] and Sunita G. Kramer[1,2]

[1]Department of Pathology and Laboratory Medicine, Robert Wood Johnson Medical School, University of Medicine and Dentistry of New Jersey, Piscataway, NJ 08854
[2]Joint Graduate Program in Cell and Developmental Biology, University of Medicine and Dentistry of New Jersey Graduate School of Biomedical Sciences and Rutgers, the State University of New Jersey, Piscataway, NJ 08854

During *Drosophila melanogaster* heart development, a lumen forms between apical surfaces of contralateral cardioblasts (CBs). We show that Slit and its receptor Roundabout (Robo) are required at CB apical domains for lumen formation. Mislocalization of Slit outside the apical domain causes ectopic lumen formation and the mislocalization of cell junction proteins, E-cadherin (E-Cad) and Enabled, without disrupting overall CB cell polarity. Ectopic lumen formation is suppressed in *robo* mutants, which indicates *robo*'s requirement for this process. Genetic evidence suggests that Robo and Shotgun (Shg)/E-Cad function together in modulating CB adhesion. *robo* and *shg/E-Cad* transheterozygotes have lumen defects. In *robo* loss-of-function or *shg/E-Cad* gain-of-function embryos, lumen formation is blocked because of inappropriate CB adhesion and an accumulation of E-Cad at the apical membrane. In contrast, *shg/E-Cad* loss-of-function or *robo* gain-of-function blocks lumen formation due to a loss of CB adhesion. Our data show that Slit and Robo pathways function in lumen formation as a repulsive signal to antagonize E-Cad–mediated cell adhesion.

Introduction

Lumen morphogenesis is an essential process during the formation of vascular tissue. Blood vessels are tubes formed by a single layer of polarized endothelial cells with junctional contacts enclosing a central lumen (Davis et al., 2000). Although several models have been proposed for lumen formation (Lubarsky and Krasnow, 2003), the cellular and molecular mechanisms that drive this process are poorly understood. The *Drosophila melanogaster* embryonic heart, a simple linear tube resembling a vertebrate capillary, provides a straightforward genetic model for vessel morphogenesis and lumen formation.

Several studies, both in vitro and in vivo, show that the vascular lumen is established via the formation of intracellular vacuoles, which fuse together with the plasma membrane to produce a lumen between cells (Vega-Salas et al., 1987; Davis and Camarillo, 1996; Beitel and Krasnow, 2000; Kamei et al., 2006). Presumably, dynamic changes in cell adhesion and cell–cell contacts must also be regulated to account for morphogenetic changes accompanying this process. The cadherin family of molecules (Carthew, 2005) plays an important role in vessel formation via both their adhesive and signaling functions (Dejana et al., 1999). In vertebrate endothelial cells, VE-cadherin is localized specifically to sites of cell contact known as adherens junctions (Bach et al., 1998; Vincent et al., 2004). Recent evidence suggests the adhesive function of cells is dynamically regulated through E-cadherin (E-Cad) endocytosis (Gumbiner, 2000). However, what remains unclear is how intracellular cell adhesion mechanisms are regulated by extracellular signals to control complex cell shape changes.

Slit is an extracellular matrix protein that is the ligand for the Roundabout (Robo) family of transmembrane receptors (Rothberg et al., 1990; Brose et al., 1999; Kidd et al., 1999). Genetic data from *D. melanogaster* and *Caenorhabditis elegans* together with in vivo studies in mice indicate a conserved role for Slit and Robo proteins in repulsive axon guidance (for review see Dickson and Gilestro, 2006). In the *D. melanogaster*

Correspondence to Sunita G. Kramer: kramersg@umdnj.edu

Abbreviations used in this paper: Baz, Bazooka; CB, cardioblast; Dlg, Discs-large; E-Cad, E-cadherin; Ena, Enabled; GOF, gain of function; LOF, loss of function; PC, pericardial cell; Robo, roundabout; Shg, shotgun; XS, cross section.

The online version of this paper contains supplemental material.

The Rockefeller University Press $30.00
J. Cell Biol. Vol. 182 No. 2 241–248
www.jcb.org/cgi/doi/10.1083/jcb.200804120

central nervous system, expression of *slit* by the midline glial cells creates a repulsive cue for *robo*-expressing central nervous system axons (Kidd et al., 1999). Here, we present genetic evidence for a repulsive activity for Slit in the heart. Specifically, we show that Slit/Robo signaling is required at the apical plasma membrane of heart cells for inhibiting E-Cad–mediated cell adhesion, thus permitting cell shape changes required for lumen formation.

Results and discussion

D. melanogaster heart lumen formation

The alignment of cardioblasts (CBs) into rows on either side of the midline is the first of several steps during heart tube assembly. After alignment, the two rows of CBs, which are each flanked by a row of pericardial cells (PCs), migrate dorsally. Prior to merging at the midline, CBs undergo a mesenchyme-to-epithelium transition and acquire apical-basal polarity (Fremion et al., 1999). At the dorsal midline, contralateral pairs of CBs make specific dorsal and ventral contacts between their opposing apical membranes to form the lumen (Fig. 1, D and H). To better understand the steps leading to lumen formation, we performed EM on cross sections (XSs) of wild-type embryos at three steps during the late stages of heart development. At early embryonic stage 16, each CB initiates contact with its contralateral counterpart at the dorsalmost leading edge of the apical membrane (Fig. 1 A). After dorsal contact, CBs undergo a shape change and make contact at their ventral apical surfaces (Fig. 1 B). In this way, a lumen is formed between two opposing CBs (Fig. 1 C). The fact that CBs specifically make contact at dorsal and ventral attachment points (Fig. 1 D) suggests that an inhibitory mechanism may prevent the centralmost apical surfaces between these points from coming into contact.

Slit and Robo are expressed in the lumen of the heart

During the early stages of heart morphogenesis (embryonic stage 14), Slit is uniformly distributed on CB surfaces (Qian et al., 2005; Santiago-Martínez et al., 2006). We reported that Slit and its receptors Robo and Robo2 play an important role in the dorsal migration of CBs and PCs (Santiago-Martínez et al., 2006). Prior to merging at the dorsal midline, Slit becomes restricted to CB apical surfaces (Santiago-Martínez et al., 2006). This dynamic change in Slit localization suggests that during this late phase of heart morphogenesis, Slit has a second function in lumen formation.

To explore the function of Slit and Robos in lumen formation, we performed a detailed analysis of Slit, Robo, and Robo2 localization in the heart, focusing on stage 17 after CB migration has occurred. Whole mount antibody staining revealed that Slit's localization is polarized at the apical surface of CBs (Fig. 1 E). Robo is also polarized at CB apical surfaces (Fig. 1 F). Robo2 is absent from the CBs and is restricted to the two rows of PCs, which flank the CBs (Fig. 1 G). To precisely localize these proteins, we performed immunohistochemistry on embryos that we examined in XS. Both Slit and Robo are localized to the CB apical surfaces surrounding the central lumen of the heart (Fig. 1, I and J). XSs also confirm that Robo2 is localized to PCs and excluded from the lumen (Fig. 1 K). The concurrent expression of Slit and Robo at CB apical surfaces suggests that these proteins may play an important role in lumen formation.

slit overexpression results in ectopic lumen formation

A notable aspect of heart tube formation is that although the dorsal and ventral leading edges of CB apical surfaces make connections with their contralateral partners, the innermost surfaces fail to come in contact (Fig. 1 D). Based upon Slit's localization at the CB apical domain and Slit's well-characterized role in repulsive guidance (Brose et al., 1999; Kidd et al., 1999; Kramer et al., 2001), we hypothesized that Slit may be responsible for preventing CB membranes from coming into contact, permitting the formation of a lumen. To test this idea, we used the Gal4-UAS system (Brand and Perrimon, 1993) to overexpress *slit* in the heart. Using the Mef-Gal4 driver to drive UAS-*slit* in a *slit* mutant background (*slit* gain of function [GOF]), we achieved rescue of the heart cell positioning phenotype in which the CBs fail to migrate to the dorsal midline of the embryo (Santiago-Martínez et al., 2006). However, at stage 16, Slit is no longer restricted to the apical surface of CBs and is now also localized basally and on the PCs as well (Fig. 2 B). In *slit* GOF embryos, Robo is now also mislocalized to CB basal surfaces (Fig. 2 D). Examination of the heart in *slit* GOF embryo XSs by EM revealed two lumens (Fig. 2 F) rather than the single lumen observed in the wild type (Fig. 2 E). We observed this phenotype in all of the embryos we sectioned ($n = 9$). The ectopic lumens were not continuous along the entire length of the heart tube but rather were confined to the pair of CBs in the section. By examining serial sections, we observed a series of disconnected lumens. Both lumens are lined with extracellular matrix, a recognizable feature in EM and shown to line the *D. melanogaster* heart (Fig. 2, G and H; Haag et al., 1999). To identify between which cell types ectopic lumens were forming, we performed Mef2 staining on *slit* GOF embryos that we examined in XS. Mef2 labels CB nuclei, and in wild-type embryos, the lumen is visible between these cells (Fig. 2 I). In *slit* GOF embryos, ectopic lumens are formed between CBs and neighboring non-Mef2–positive PC or amnioserosal cells (Fig. 2 J). These results demonstrate that when Slit is no longer polarized, CBs are impaired in their ability to confine formation of the lumen to their apical domains.

Lumen defects in *slit* GOF are not caused by the loss of apicobasal polarity

We hypothesize that Slit localization correlates with lumen formation because of the selective repulsion of CB membranes. However, an alternative explanation may be that lumen defects in *slit* GOF embryos are secondary to general defects in CB polarity. In *slit* embryos, the rows of CBs do not assemble properly and exhibit abnormal localization of several cell polarity markers (Qian et al., 2005; Santiago-Martínez et al., 2006). To confirm that the *slit* GOF phenotype was not secondary to defects in cell polarity, we examined cell polarity markers in these embryos. Discs-large (Dlg), a membrane-associated guanylate

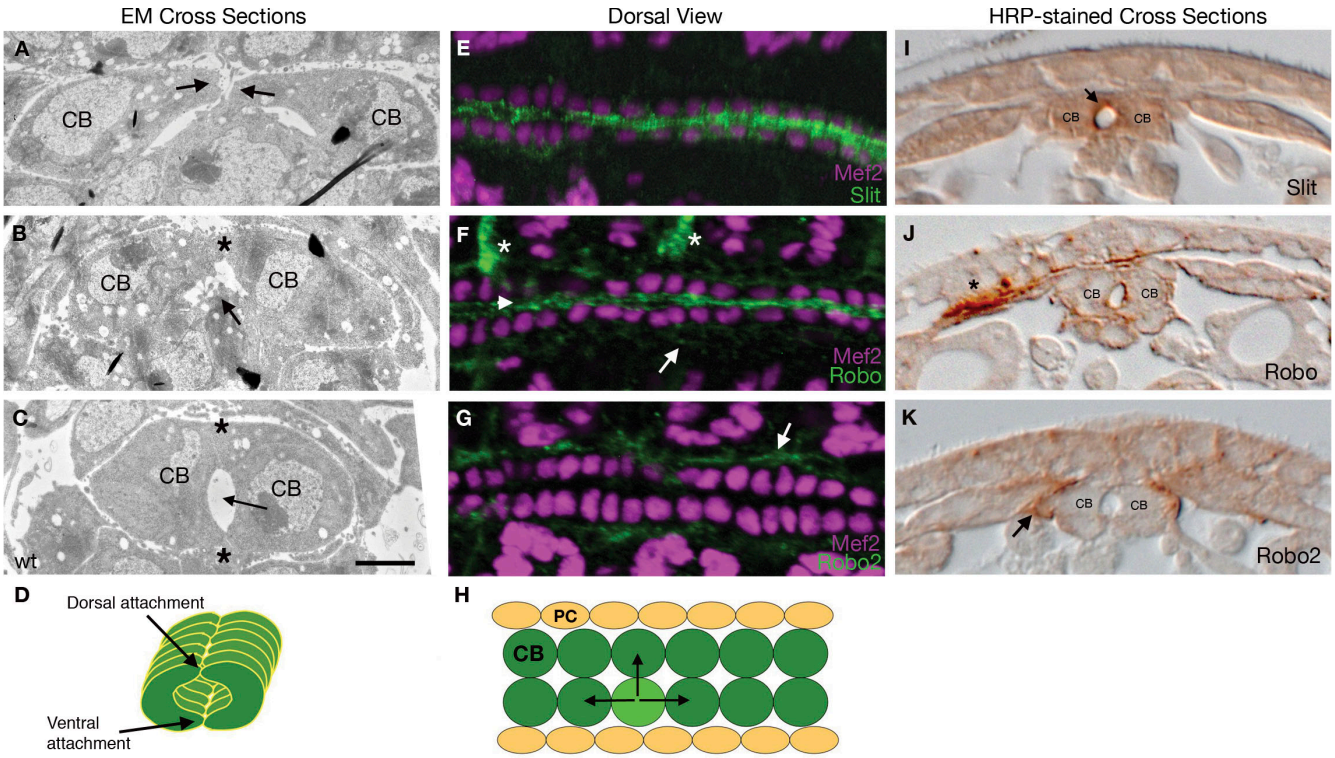

Figure 1. **Localization of Slit, Robo, and Robo2 in the heart.** All embryos are wild type. (A–C) EMs of embryos in XS. (A) Early stage 16 embryo showing two CBs initiating contact at their dorsal leading edges (arrows). (B) At late stage16, the dorsal edge has made contact (asterisk) and the CBs are initiating contact ventrally (arrow). (C) At stage 17, the lumen (arrow) is formed between two contralateral CBs joined at dorsal and ventral attachment points (asterisks). (D) Schematic of the heart in XS showing CBs joined at dorsal and ventral attachments (arrows). (E–G) Confocal images of stage 16 embryos in a dorsal view. (E) Mef2 labels CB nuclei (magenta), and Slit (green) localizes to the apical side of CBs. (F) Mef2 (magenta) and Robo (green). Robo localizes to the apical side of CBs, alary muscles (asterisks), and PCs (arrow). (G) Mef2 (magenta) and Robo2 (green), which localizes to the PCs (arrow). (H) Schematic of the heart in dorsal view showing the position of CBs (green) and PCs (yellow). A single CB is shown making contact with one contralateral and two ipsilateral CBs (arrows). (I–K) XSs of stage 17 embryos stained with HRP (brown). (I) Slit accumulates at the apical surface of the lumen (arrow). (J) Robo localizes to apical lumenal surface and the alary muscles (asterisk). (K) Robo2 is restricted to the PCs (arrow). Bar, 2 µm.

kinase protein (Woods et al., 1996), normally localizes to the apical-lateral surface of CBs in stage 16 embryos (Fig. S1 A, available at http://www.jcb.org/cgi/content/full/jcb.200804120/DC1). In *slit GOF* embryos, this pattern is not significantly altered (Fig. S1 B), which indicates that the CBs are correctly polarized. In addition, the localization of α-spectrin, a membrane-bound cytoskeletal protein (Lee et al., 1993) that preferentially localizes to the basal-lateral surface of CBs (Santiago-Martínez et al., 2006), was normal in *slit* GOF embryos (Fig. S1 G).

robo is required for lumen formation

In embryos mutant for *slit* or both *robo* and *robo2*, the rows of CBs do not properly align, resulting in gaps at the dorsal midline (Santiago-Martínez et al., 2006). It has been found that *slit* mutant embryos have lumen defects (MacMullin and Jacobs, 2006). However, because of the severe CB alignment phenotype in *slit* or *robo*,*robo2* mutants, we found it difficult to separate *slit*'s earlier role in ipsilateral CB cell alignment with what we believe to be a later role lumen formation between contralateral CBs. Embryos mutant for *robo* alone have very mild migration defects, and the majority of CBs are able to align at the dorsal midline (Santiago-Martínez et al., 2006). EM of *robo* mutants (n = 11) reveals that contralateral CBs are inappropriately adhered, and the lumen fails to form between these cells (Fig. 3 D). In addition, Slit is no longer concentrated at CB apical domains (Fig. 3 C), which suggests that the Robo localization is important for the polarized accumulation of Slit. Moreover, the mislocalization of Slit in a *robo* mutant is not sufficient to induce ectopic lumen formation as in *slit* GOF embryos (Fig. 2 F), which suggests that Robo is required for this process. To further explore the functional connection between Slit and Robo, we show that removal of *robo* in *slit GOF* embryos completely suppresses the *slit GOF* phenotype and blocks lumen formation (Fig. 3, E and E′). Finally, we found that Dlg and α-spectrin are properly localized in *robo* mutants (Fig. S1, E and J), providing additional evidence that during lumen formation, Slit and Robo are not required for CB cell polarity but instead function at a later step once the initial polarity of the cell has already been established.

Shotgun (*shg*)/*E-Cad* is required for CB attachment

One of the only genes known to affect lumen formation in the *D. melanogaster* heart is *shg*, which encodes E-Cad. (Tepass et al., 1996; Uemura et al., 1996). It was previously shown that E-Cad is expressed by the CBs, and that in *shg* mutants, the rows of CBs align but fail to attach to each other across the midline (Haag et al., 1999). We further investigated these findings by first examining the localization of E-Cad in cross-sectioned

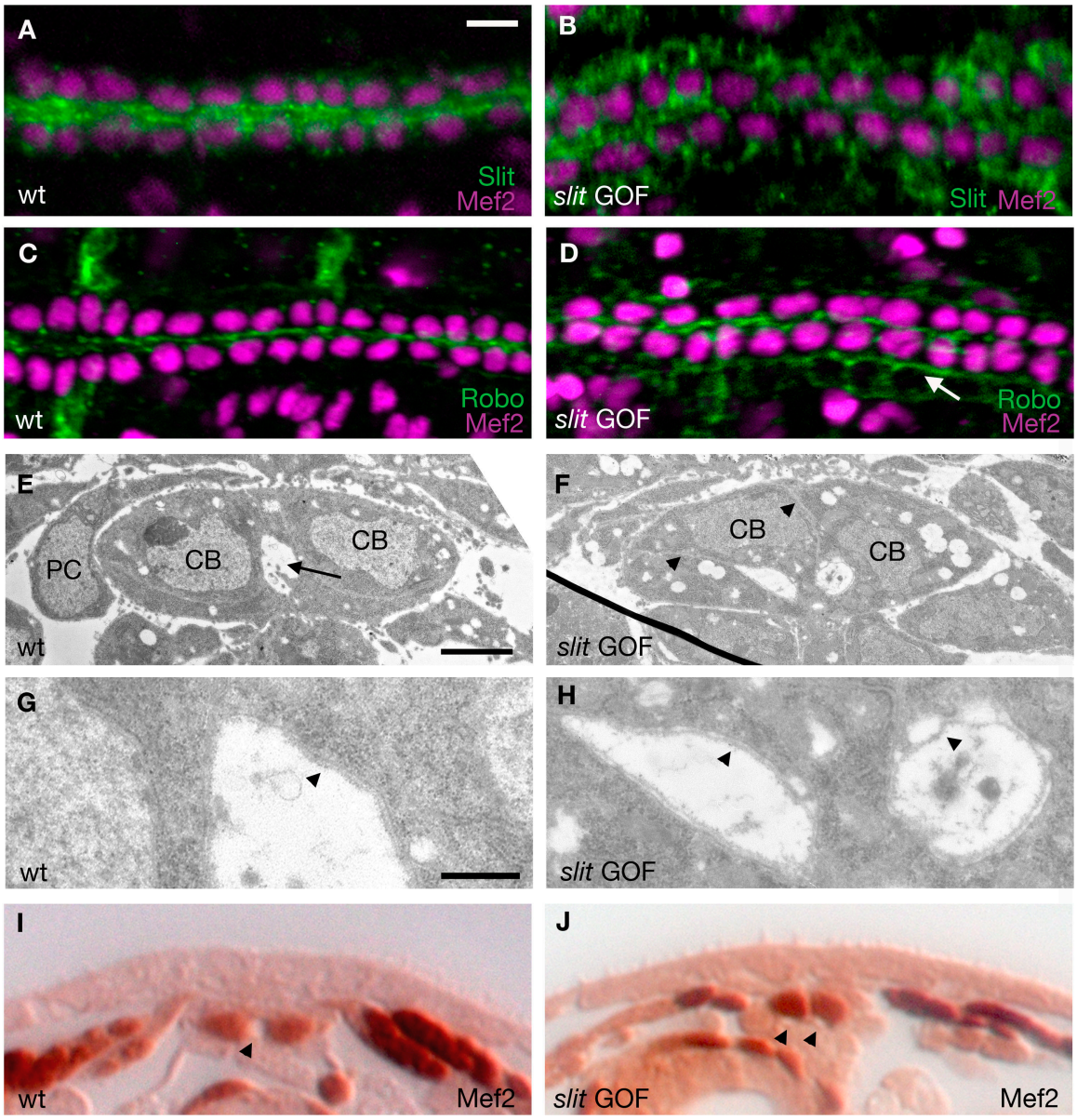

Figure 2. **Overexpression of *slit* results in ectopic lumen formation.** All embryos are stage 17. (A–D) Dorsal view of embryos stained for Mef2 (magenta), which labels CB nuclei, and Slit or Robo (green). (A) A wild-type embryo showing the normal pattern of Slit. (B) *slit* embryo with one copy each of *Mef-Gal4* and *UAS-slit* (*slit* GOF) in which Slit is no longer restricted to the CB apical domains. (C) Wild type pattern of Robo. (D) Robo is mislocalized to CB basal surfaces (arrow) in a *slit* GOF embryo. (E) EM of a wild-type embryo in XS showing the lumen (arrow) that forms between two CBs. (F) EM of a *slit* GOF embryo showing the two-lumen phenotype. Arrowheads indicate cell membranes. (G and H) Close up views of E and F. Arrowheads indicate the extracellular matrix. (I and J) XSs of embryos stained for Mef2, which labels CB and somatic muscle nuclei (brown). (I) The lumen is visible between CBs (arrowhead) in a wild-type embryo. (J) *slit* GOF embryo with two lumens (arrowheads). Bars: (A) 6 µm; (E) 2 µm; (G) 0.5 µm.

embryos. In stage 17 embryos, E-Cad is concentrated at the dorsal and ventral sites of contact between opposing pairs of CBs (Fig. 3 F). Next, we examined the lumen in *shg/E-Cad* mutants by EM ($n = 2$). In *shg/E-Cad* mutants, CBs fail to attach and form a lumen (Fig. 3 G), and we observed the presence of extracellular space between contralateral CBs (Fig. 3 H).

robo and *shg/E-Cad* interactions

The loss of CB adhesion in *shg/E-Cad* mutants (Fig. 3 H) is interesting in comparison to *robo* mutants, in which CBs are inappropriately adhered along the entire apical face (Fig. 3 H′). These results suggest that *robo* and *shg/E-Cad* play opposing roles in lumen formation. Robo functions to prevent the CBs from sticking together at the central apical surfaces of the CBs, whereas E-Cad is required to maintain cell adhesion dorsally and ventrally. To further investigate their combined functions, we tested for genetic interactions by examining the lumen in embryos transheterozygous for *robo* and *shg/E-Cad*. Although genetic interactions between *slit* and *shg/E-Cad* during the earlier step of CB alignment have been explored (Qian et al., 2005), it remains to be shown whether *shg/E-Cad* interacts specifically with *robo* during lumen formation. Embryos that were missing a single copy of either *robo* or *shg/E-Cad* did not have obvious lumen defects (unpublished data). However, in 89% of *robo/shg* transheterozygotes

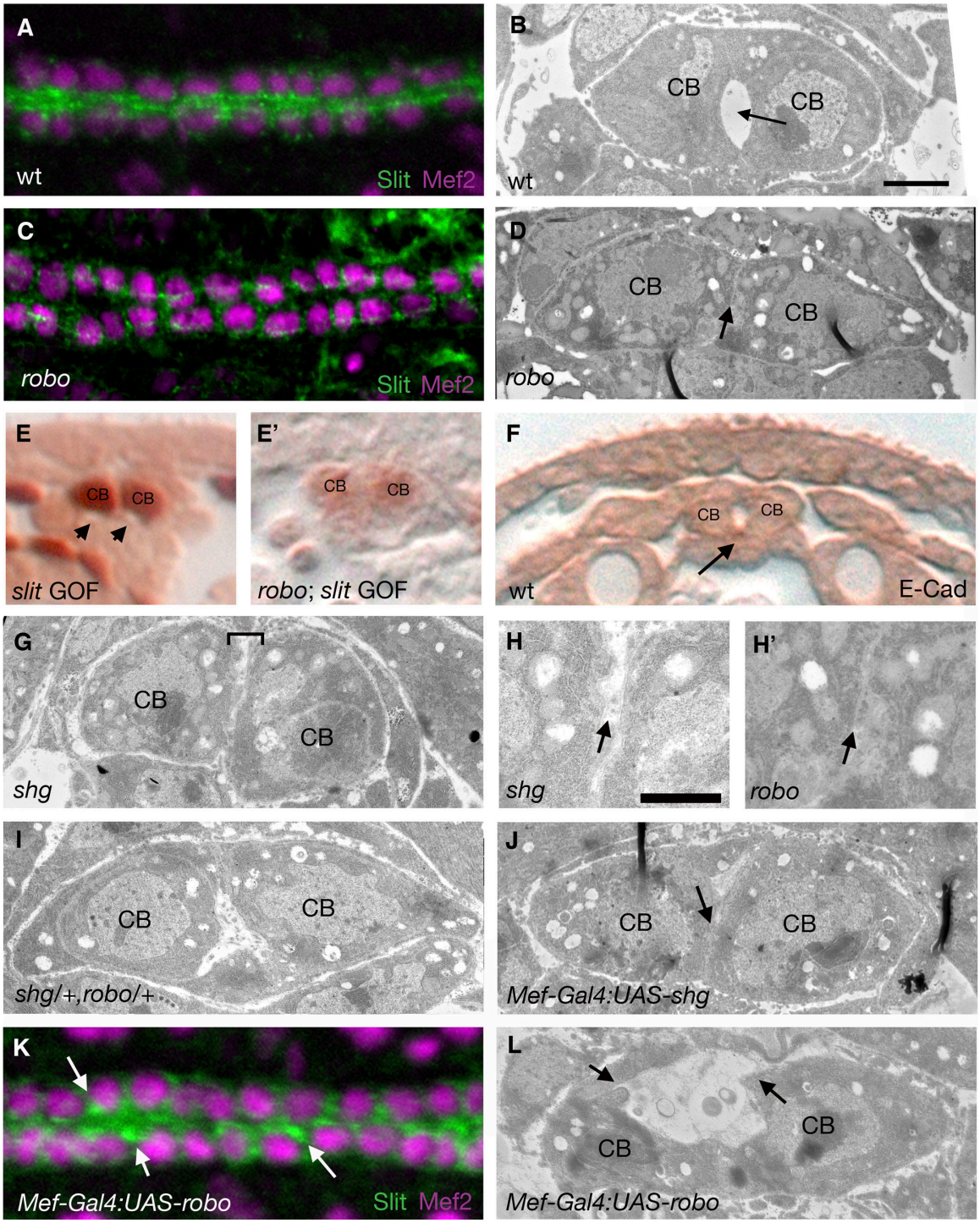

Figure 3. **LOF and GOF phenotypes in the heart.** All embryos are stage 17. (A) Dorsal view of a wild-type embryo stained for Mef2 (magenta) and Slit (green). (B) EM of a wild-type heart in XS showing the lumen between two CBs (arrow). (C) *robo* embryo stained for Slit (green) and Mef2 (magenta). (D) EM of a *robo* embryo showing a block in lumen formation. Arrow indicates the region where the CBs remain inappropriately attached. (E) XS of a *slit* GOF embryo stained with anti-Mef2, which labels CB nuclei. Two lumens are visible (arrowheads). (E') Removal of *robo* in a *slit* GOF background suppresses the two-lumen phenotype. (F) Anti–E-Cad staining in the wild-type heart. Staining at the ventral attachment point is marked with an arrow. (G) EM of *shg/E-Cad* mutant shows that CBs fail to attach to each other (bracket). (H and H') Close up of EMs in G and D. In *robo* embryos (H'), the CBs are closely associated (arrow), as compared with *shg/E-Cad* mutants (H), where the cells fail to adhere, as indicated by the presence of extracellular space between CBs (arrow). (I) EM of a *shg/+,robo/+* embryo showing defects in lumen formation. (J) EM of a *Mef-Gal4/+;UAS-shg/+* embryo showing that lumen formation is blocked (arrow). (K) *Mef-Gal4/+;UAS-robo/+* embryo stained for Slit (green) and Mef2 (magenta). Slit is localized to the apical domain of CBs but the staining is nonuniform (arrows). (L) EM of a *Mef-Gal4/+;UAS-robo/+* embryo in which the CBs have lost their dorsal point of attachment (arrows). Bars: (B) 2 µm; (H) 1 µm.

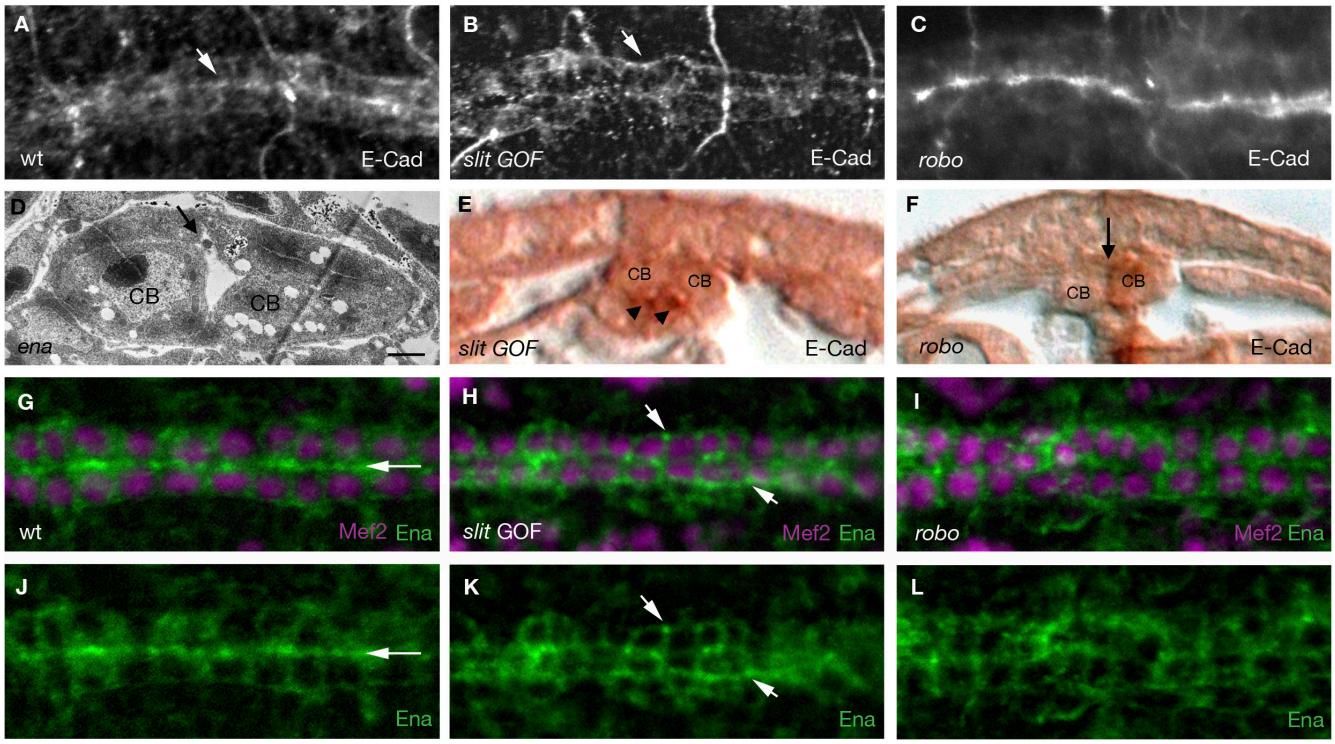

Figure 4. **Examination of cell junction markers.** All embryos are stage 17. (A) E-Cad localizes to CB apical surfaces (arrow). (B) In *slit* GOF embryos, E-Cad is also localized to CB basal surfaces (arrow). (C) In *robo* mutants, E-Cad accumulates at high levels at CB apical domains. (D) EM of an *ena* mutant. Arrow indicates a region where CBs fail to make contact. (E and F) E-Cad staining in cross-sectioned embryos as visualized by HRP staining. (E) in *slit* GOF embryos, E-Cad is enriched at sites of cell contact in both lumens (arrowheads). (F) In *robo* mutants, E-Cad accumulates at apical domains where CBs remain in contact (arrow). (G–I) Mef2 (magenta) and Ena (green), which concentrates at CB apical surfaces (arrow) in wild-type embryos (G). In *slit* GOF embryos (H), Ena is mislocalized to CB basal and lateral domains in discrete puncta (arrows). (I) In *robo* mutants, Ena is no longer concentrated at the apical domain of CBs. (J–L) Same as G–I showing Ena alone. Bar, 1 μm.

($n = 9$), the lumen was misshapen (Fig. 3 I), which suggests that the functions of *robo* and *shg/E-Cad* are linked.

Next, we took a GOF approach to investigate the respective roles of *robo* and *shg/E-Cad* during lumen formation. When we overexpressed *shg/E-Cad* in the CBs using Mef-Gal4, we observed significant heart defects. However, unlike what we observed in *shg/E-Cad* mutants where the CBs failed to attach (Fig. 3 G), the failure in lumen formation in *shg/E-Cad* GOF embryos is caused by the inappropriate adhesion of contralateral CBs. By EM, we observe CBs that are inappropriately attached with no extracellular space in between ($n = 9$; Fig. 3 J). We also found that Dlg and α-spectrin were properly localized (Fig. S1, D and I), which indicates that the defects were not secondary to loss of CB cell polarity.

robo loss of function (LOF) embryos have a phenotype similar to *shg/E-Cad* GOF embryos, in which CBs are inappropriately attached (Fig. 3, D and H′). We hypothesize that Robo's function at this stage is to repel contralateral CBs at the central apical domain, enabling the formation of a lumen in this region. Consistent with this idea, we found that overexpression of *robo* in CBs using Mef-Gal4 results in severe lumen defects. Although CBs were properly aligned (Fig. 3 K) and polarized (Fig. S1, C and H), with EM ($n = 5$), we observed a loss of cell contact between the dorsal and/or ventral CB apical surfaces (Fig. 3 L). These results indicate that high levels of Robo prevent CBs from initiating or maintaining adhesion at the specific sites of contact and suggest that *robo* overexpression can overcome E-Cad–mediated cell adhesion at these sites. Interestingly, in *robo* GOF embryos we found that although Slit remains polarized in CBs, we see Slit staining in intense patches (Fig. 3 K) as compared with more uniform localization in the wild type (Fig. 3 A).

Mislocalization of E-Cad and Bazooka (Baz) in *slit GOF* or *robo* LOF embryos

Based upon our findings, we hypothesize that Slit and Robo function to negatively regulate E-Cad–mediated cell adhesion between opposing CBs. Next, we examined the localization of E-Cad in our mutant backgrounds. In the wild type, E-Cad localizes to the specific sites of cell–cell contact between contralateral CBs (Fig. 3 F). The concentration of E-Cad at CB apical membranes can also be seen in dorsal view (Fig. 4 A). In *slit* GOF embryos where we observe ectopic lumen formation, we noticed changes in E-Cad expression. E-Cad fails to accumulate at high levels at the apical domain in CBs (Fig. 4 B). In XS, ectopic E-Cad accumulation is seen at sites of cell–cell contact surrounding the ectopic lumens (Fig. 4 E). However, in *robo* mutants, we observed higher–than–wild type levels of E-Cad at the apical membrane as seen in dorsal view and in XS (Fig. 4, C and F). These results are consistent with our EM studies revealing that in *robo* mutants, the CBs are tightly adhered (Fig. 3 H′). We obtained similar results when we looked at Baz localization (Fig. S1, K–O). Baz is a PDZ domain–containing protein that may provide a landmark for

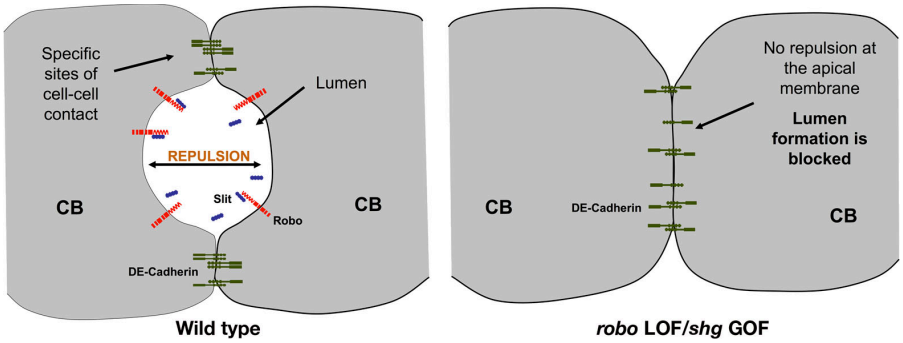

Figure 5. **Summary of heart tube lumen formation in wild-type and mutant embryos.** Lumen formation in the *D. melanogaster* heart depends on specific sites of adhesion and de-adhesion between contralateral CBs. We propose that Slit/Robo signaling is required to maintain de-adhesion along the central apical domain of contralateral CBs. In wild-type embryos, CBs are specifically adhered at dorsal and ventral attachment points where E-Cad accumulates. Between these points, the apical membranes of the CBs are repelled from each other, allowing for the formation of a lumen. In *robo* LOF or *shg/E-Cad* GOF embryos, contralateral CBs remain adhered to each other, resulting in a block in lumen formation and an apical accumulation of E-Cad.

adherens junction assembly by recruiting E-Cad to sites of cell–cell contact (Harris and Peifer, 2005).

Changes in Enabled (Ena) localization in *slit GOF* or *robo* LOF embryos

The Ena/VASP family of proteins regulate actin dynamics during cell motility (Krause et al., 2003) and, more recently, has been implicated in cell adhesion (Vasioukhin et al., 2000; Grevengoed et al., 2001; Scott et al., 2006). Here, we find that Ena, similar to E-Cad and Baz, is localized at the apical domain of CBs in regularly spaced puncta (Fig. 4, G and J). In *robo* mutants, Ena is no longer concentrated at CB apical domains (Fig. 4, I and L). Embryos mutant for *ena* have lumen defects as observed by EM ($n = 4$) that are consistent with a loss of CB cell contact (Fig. 4 D). What is the function of Ena during lumen formation? One possibility is that, similar to its role during *D. melanogaster* dorsal closure (Gates et al., 2007), Ena may be required for protrusive behavior of the CBs to permit cell–cell contact. Alternatively, Ena may be required for regulating E-Cad–based adhesion. This hypothesis is supported by our findings that Ena localizes to ectopic sites along CB basal surfaces in *slit* GOF embryos (Fig. 4, H and K), where we observe ectopic sites of E-Cad localization (Fig. 4, B and E). Interestingly, Ena has been shown to directly interact with Robo to mediate repulsive signaling during axon guidance (Bashaw et al., 2000). Our data suggest that Ena may provide a critical link between Robo and E-Cad during lumen formation, and provide an avenue for further study.

For *D. melanogaster* heart lumen formation, CBs must be attached at specific sites but also have apical surfaces that are not adhered (Fig. 5). Our studies show that Slit/Robo signaling is required for lumen formation between CBs by inhibiting E-Cad–mediated cell adhesion. Slit and Robo localize to the apical surface of the CBs facing the lumen. In *robo* LOF or *shg/E-Cad* GOF embryos, contralateral CBs are tightly bound, resulting in a failure of lumen formation (Fig. 5). However, when Slit is ectopically expressed on basal and lateral surfaces, we observe an inappropriate loss of cell adhesion in these regions, resulting in the formation of ectopic lumens (Fig. 2, F and H). These phenotypes are accompanied by mislocalization of the cell junction markers E-Cad, Ena (Fig. 4), and Baz (Fig. S1) to these sites. How might Slit and Robo regulate cell adhesion and lumen formation? Much of our understanding of Slit and Robo signaling has emerged from studies of how Robo's activation by Slit regulates downstream cytoskeletal changes during axon guidance (Dickson and Gilestro, 2006). Two recent in vitro studies support our findings that, in addition to their known role in cell migration, Robo proteins also function to either positively or negatively regulate cell adhesion (Rhee et al., 2002; Kaur et al., 2006). Here, we provide in vivo genetic evidence that Slit and Robo negatively regulate cell adhesion during lumen formation. The next step will be to identify the downstream mechanisms by which Slit and Robo signaling negatively regulate E-Cad–mediated cell adhesion.

Materials and methods

D. melanogaster genetics

Fly crosses and experiments were performed at 25°C. The w^{1118} strain was used as the wild type. The following mutations have been described previously: null alleles for *slit* (sli^1,sli^2) and *robo* ($robo^{2570}$, $robo^5$; Kidd et al., 1999). *UAS-slit* and UAS-*robo* were also described previously (Kramer et al., 2001). The UAS-GAL4 system was used to drive expression of the *slit* transgene with Mef-GAL4. *$slit^2$/Cyo,pActGFP;UAS-slit* was crossed with *sli^2/Cyo,pActGFP; Mef-GAL4* to get *$slit^2$/$slit^2$; Mef-Gal4/UAS-slit* embryos. *sli^1,$robo^5$/Cyo,WgBgal; Mef-Gal4* was crossed with *sli^1,$robo^5$/Cyo,WgBgal; UAS-slit* to get *sli^1,$robo^5$/ sli^1,$robo^5$; Mef-Gal4/UAS-slit* embryos. The ena allele used was ena^{23} (BL stock No. 8571) and the *shg/E-Cad* allele used in this study was shg^{K03401} (BL stock No. 10377); they were obtained from the Bloomington Stock Center. The wild-type *UAS-shg* transgene (Oda and Tsukita, 1999) was obtained from the Drosophila Genetic Resource Center (Kyoto Institute of Technology).

Immunofluorescence

Embryos were fixed and stained as described previously (Santiago-Martínez et al., 2006). The following antibodies were used: mouse anti-Slit (1:10), mouse anti-Robo (1:10) and rabbit anti-Robo2 (1:1,000; 16), rabbit anti-Mef2 (1:2,000; a gift from B. Paterson, National Cancer Institute, National Institutes of Health, Bethesda, MD), and rabbit anti-Baz (1:1,000; gift from A. Wodarz; University of Göttingen, Göttingen, Germany). Mouse anti-Dlg (1:10), mouse anti-Enabled (1:10), mouse anti–α-spectrin (1:10), rat anti–DE-cadherin (1:10; obtained from the Developmental Studies Hybridoma Bank, developed under the auspices of the National Institute of Child Health and Human Development, and maintained by the University of Iowa), FITC anti–mouse (1:500), Alexa 488 anti–rabbit (1:500), Cy3 anti–mouse (1:500) and –rabbit (1:500), Biotin anti–rat (1:500) and Streptavidin 488 (Invitrogen), and anti–β-Gal (1:10,000; MP Biomedicals). Embryos were mounted in Vectashield mounting media for fluorescence (Vector Laboratories), and confocal z sections were collected at ambient temperature on a microscope (IX81; Olympus) with a CARV Nipkow disc confocal unit (BD Biosciences) equipped with a VApo/340 40× 1.15 NA water immersion objective (Olympus) and a SensiCam QE camera (the Cooke Corporation). Image processing and analysis was done with IPLab image analysis software (BD Biosciences) and Photoshop CS2 (Adobe).

EM

Mutant embryos were selected based on the absence of GFP-marked balancer chromosome. Embryos were fixed and embedded as described previously

(Santiago-Martínez et al., 2006). 90-nm sections were cut using a microtome (Ultracut E; Leica) from the posterior to the anterior end of the embryo and picked up on a copper or a carbon support film on specimen grids. Sections were stained with uranyl acetate and lead citrate. XSs were examined and using an electron microscope (CM-12; Philips) operating at 80 kV. Digital images were collected using a digital camera (XR611/BZ; Advanced Microscopy Techniques) and Image Capture Engine V600 software (Advanced Microscope Techniques) and processed using Photoshop CS2 (Adobe).

Immunohistochemistry

Embryos were fixed and stained at ambient temperature using anti-Slit, anti-Robo, anti-Robo2, anti-Mef2, and anti–E-Cad as described previously (Santiago-Martínez et al., 2006). Biotin and conjugated streptavidin-HRP (Invitrogen) were used as secondary antibodies, and the signal was enhanced using a Metal Enhanced DAB Substrate kit (Pierce). Embryos were staged and embedded in epon-Spurr resin. 4-µm sections were cut using the Ultracut E microtome from the posterior to the anterior end of the embryo and subsequently imaged on a Axio Imager.A1 equipped with a Plan-APO 40× 0.95 NA objective and an AxioCam MRc5 digital camera (all from Carl Zeiss, Inc.). Image processing and analysis was done with AxioVision 4.6 (Carl Zeiss, Inc.) and Photoshop CS2 (Adobe) software.

Online supplemental material

Fig. S1 shows the expression of the cell polarity markers Dlg and α-spectrin and the cell junctional marker Baz in wild-type, *slit* GOF, *robo* GOF, *shg* GOF, and *robo* LOF backgrounds. Online supplemental material is available at http://www.jcb.org/cgi/content/full/jcb.200804120/DC1.

We thank Kevin Ang for assistance with embryo stainings, Jeff Roberto for assistance with line art, and Colleen Guerin, Raymond Habas, Joe Kramer, Haichang Li, Ramani Ranchandran, and William Wadsworth for helpful discussions and critical reading of the manuscript.

This study was supported by a Scientist Development Grant from the American Heart Association (0435395T) and a National Science Foundation grant (award ID 0744165) to S.G. Kramer, and a National Institutes of Health Predoctoral Fellowship (F31/GM75393) to E. Santiago-Martínez.

Submitted: 21 April 2008
Accepted: 11 June 2008

References

Bach, T.L., C. Barsigian, D.G. Chalupowicz, D. Busler, C.H. Yaen, D.S. Grant, and J. Martinez. 1998. VE-Cadherin mediates endothelial cell capillary tube formation in fibrin and collagen gels. *Exp. Cell Res.* 238:324–334.

Bashaw, G.J., T. Kidd, D. Murray, T. Pawson, and C.S. Goodman. 2000. Repulsive axon guidance: Abelson and Enabled play opposing roles downstream of the roundabout receptor. *Cell.* 101:703–715.

Beitel, G.J., and M.A. Krasnow. 2000. Genetic control of epithelial tube size in the *Drosophila* tracheal system. *Development.* 127:3271–3282.

Brand, A.H., and N. Perrimon. 1993. Targeted gene expression as a means of altering cell fates and generating dominant phenotypes. *Development.* 118:401–415.

Brose, K., K.S. Bland, K.H. Wang, D. Arnott, W. Henzel, C.S. Goodman, M. Tessier-Lavigne, and T. Kidd. 1999. Slit proteins bind Robo receptors and have an evolutionarily conserved role in repulsive axon guidance. *Cell.* 96:795–806.

Carthew, R.W. 2005. Adhesion proteins and the control of cell shape. *Curr. Opin. Genet. Dev.* 15:358–363.

Davis, G.E., and C.W. Camarillo. 1996. An alpha 2 beta 1 integrin-dependent pinocytic mechanism involving intracellular vacuole formation and coalescence regulates capillary lumen and tube formation in three-dimensional collagen matrix. *Exp. Cell Res.* 224:39–51.

Davis, G.E., S.M. Black, and K.J. Bayless. 2000. Capillary morphogenesis during human endothelial cell invasion of three-dimensional collagen matrices. *In Vitro Cell. Dev. Biol. Anim.* 36:513–519.

Dejana, E., G. Bazzoni, and M.G. Lampugnani. 1999. Vascular endothelial (VE)-cadherin: only an intercellular glue? *Exp. Cell Res.* 252:13–19.

Dickson, B.J., and G.F. Gilestro. 2006. Regulation of commissural axon pathfinding by slit and its Robo receptors. *Annu. Rev. Cell Dev. Biol.* 22:651–675.

Fremion, F., M. Astier, S. Zaffran, A. Guillen, V. Homburger, and M. Semeriva. 1999. The heterotrimeric protein Go is required for the formation of heart epithelium in *Drosophila*. *J. Cell Biol.* 145:1063–1076.

Gates, J., J.P. Mahaffey, S.L. Rogers, M. Emerson, E.M. Rogers, S.L. Sottile, D. Van Vactor, F.B. Gertler, and M. Peifer. 2007. Enabled plays key roles in embryonic epithelial morphogenesis in *Drosophila*. *Development.* 134:2027–2039.

Grevengoed, E.E., J.J. Loureiro, T.L. Jesse, and M. Peifer. 2001. Abelson kinase regulates epithelial morphogenesis in *Drosophila*. *J. Cell Biol.* 155:1185–1198.

Gumbiner, B.M. 2000. Regulation of cadherin adhesive activity. *J. Cell Biol.* 148:399–404.

Haag, T.A., N.P. Haag, A.C. Lekven, and V. Hartenstein. 1999. The role of cell adhesion molecules in *Drosophila* heart morphogenesis: faint sausage, shotgun/DE-cadherin, and laminin A are required for discrete stages in heart development. *Dev. Biol.* 208:56–69.

Harris, T.J., and M. Peifer. 2005. The positioning and segregation of apical cues during epithelial polarity establishment in *Drosophila*. *J. Cell Biol.* 170:813–823.

Kamei, M., W.B. Saunders, K.J. Bayless, L. Dye, G.E. Davis, and B.M. Weinstein. 2006. Endothelial tubes assemble from intracellular vacuoles in vivo. *Nature.* 442:453–456.

Kaur, S., M.D. Castellone, V.M. Bedell, M. Konar, J.S. Gutkind, and R. Ramchandran. 2006. Robo4 signaling in endothelial cells implies attraction guidance mechanisms. *J. Biol. Chem.* 281:11347–11356.

Kidd, T., K.S. Bland, and C.S. Goodman. 1999. Slit is the midline repellent for the robo receptor in *Drosophila*. *Cell.* 96:785–794.

Kramer, S.G., T. Kidd, J.H. Simpson, and C.S. Goodman. 2001. Switching repulsion to attraction: changing responses to slit during transition in mesoderm migration. *Science.* 292:737–740.

Krause, M., E.W. Dent, J.E. Bear, J.J. Loureiro, and F.B. Gertler. 2003. Ena/VASP proteins: regulators of the actin cytoskeleton and cell migration. *Annu. Rev. Cell Dev. Biol.* 19:541–564.

Lee, J.K., R.S. Coyne, R.R. Dubreuil, L.S. Goldstein, and D. Branton. 1993. Cell shape and interaction defects in α-spectrin mutants of *Drosophila melanogaster*. *J. Cell Biol.* 123:1797–1809.

Lubarsky, B., and M.A. Krasnow. 2003. Tube morphogenesis: making and shaping biological tubes. *Cell.* 112:19–28.

MacMullin, A., and J.R. Jacobs. 2006. Slit coordinates cardiac morphogenesis in *Drosophila*. *Dev. Biol.* 293:154–164.

Oda, H., and S. Tsukita. 1999. Nonchordate classic cadherins have a structurally and functionally unique domain that is absent from chordate classic cadherins. *Dev. Biol.* 216:406–422.

Qian, L., J. Liu, and R. Bodmer. 2005. Slit and Robo control cardiac cell polarity and morphogenesis. *Curr. Biol.* 15:2271–2278.

Rhee, J., N.S. Mahfooz, C. Arregui, J. Lilien, J. Balsamo, and M.F. VanBerkum. 2002. Activation of the repulsive receptor Roundabout inhibits N-cadherin-mediated cell adhesion. *Nat. Cell Biol.* 4:798–805.

Rothberg, J.M., J.R. Jacobs, C.S. Goodman, and S. Artavanis-Tsakonas. 1990. slit: an extracellular protein necessary for development of midline glia and commissural axon pathways contains both EGF and LRR domains. *Genes Dev.* 4:2169–2187.

Santiago-Martínez, E., N.H. Soplop, and S.G. Kramer. 2006. Lateral positioning at the dorsal midline: Slit and Roundabout receptors guide *Drosophila* heart cell migration. *Proc. Natl. Acad. Sci. USA.* 103:12441–12446.

Scott, J.A., A.M. Shewan, N.R. den Elzen, J.J. Loureiro, F.B. Gertler, and A.S. Yap. 2006. Ena/VASP proteins can regulate distinct modes of actin organization at cadherin-adhesive contacts. *Mol. Biol. Cell.* 17:1085–1095.

Tepass, U., E. Gruszynski-DeFeo, T.A. Haag, L. Omatyar, T. Torok, and V. Hartenstein. 1996. shotgun encodes *Drosophila* E-cadherin and is preferentially required during cell rearrangement in the neurectoderm and other morphogenetically active epithelia. *Genes Dev.* 10:672–685.

Uemura, T., H. Oda, R. Kraut, S. Hayashi, Y. Kotaoka, and M. Takeichi. 1996. Zygotic *Drosophila* E-cadherin expression is required for processes of dynamic epithelial cell rearrangement in the *Drosophila* embryo. *Genes Dev.* 10:659–671.

Vasioukhin, V., C. Bauer, M. Yin, and E. Fuchs. 2000. Directed actin polymerization is the driving force for epithelial cell-cell adhesion. *Cell.* 100:209–219.

Vega-Salas, D.E., P.J. Salas, and E. Rodriguez-Boulan. 1987. Modulation of the expression of an apical plasma membrane protein of Madin-Darby canine kidney epithelial cells: cell-cell interactions control the appearance of a novel intracellular storage compartment. *J. Cell Biol.* 104:1249–1259.

Vincent, P.A., K. Xiao, K.M. Buckley, and A.P. Kowalczyk. 2004. VE-cadherin: adhesion at arm's length. *Am. J. Physiol. Cell Physiol.* 286:C987–C997.

Woods, D.F., C. Hough, D. Peel, G. Callaini, and P.J. Bryant. 1996. Dlg protein is required for junction structure, cell polarity, and proliferation control in *Drosophila* epithelia. *J. Cell Biol.* 134:1469–1482.